FULL PAPER

Magnetic Resonance in Medicine

Multi-organ comparison of flow-based arterial spin labeling techniques: Spatially non-selective labeling for cerebral and renal perfusion imaging

Suzanne L. Franklin[1,2,3] (iD) | Isabell K. Bones[2] (iD) | Anita A. Harteveld[2] (iD) |
Lydiane Hirschler[1,3] (iD) | Marijn van Stralen[2] | Qin Qin[4] (iD) | Anneloes de Boer[2] |
Johannes M. Hoogduin[2] (iD) | Clemens Bos[2] (iD) | Matthias J. P. van Osch[1,3] (iD) |
Sophie Schmid[1,3] (iD)

[1]C.J. Gorter Center for High Field MRI, Department of Radiology, Leiden University Medical Center, Leiden, The Netherlands

[2]Center for Image Sciences, University Medical Center Utrecht, Utrecht, The Netherlands

[3]Leiden Institute for Brain and Cognition, Leiden University, Leiden, The Netherlands

[4]The Russell H. Morgan Department of Radiology and Radiological Science, Division of MR Research, Johns Hopkins University School of Medicine, Baltimore, Maryland, USA

Correspondence
Suzanne L. Franklin, C.J. Gorter Center for High Field MRI, Department of Radiology, Leiden University Medical Center, Leiden, The Netherlands.
Email: s.l.franklin@lumc.nl

Funding information
Stichting voor de Technische Wetenschappen, Grant/Award Number: 14951

Purpose: Flow-based arterial spin labeling (ASL) techniques provide a transit-time insensitive alternative to the more conventional spatially selective ASL techniques. However, it is not clear which flow-based ASL technique performs best and also, how these techniques perform outside the brain (taking into account eg, flow-dynamics, field-inhomogeneity, and organ motion). In the current study we aimed to compare 4 flow-based ASL techniques (ie, velocity selective ASL, acceleration selective ASL, multiple velocity selective saturation ASL, and velocity selective inversion prepared ASL [VSI-ASL]) to the current spatially selective reference techniques in brain (ie, pseudo-continuous ASL [pCASL]) and kidney (ie, pCASL and flow alternating inversion recovery [FAIR]).

Methods: Brain ($n = 5$) and kidney ($n = 6$) scans were performed in healthy subjects at 3T. Perfusion-weighted signal (PWS) maps were generated and ASL techniques were compared based on temporal SNR (tSNR), sensitivity to perfusion changes using a visual stimulus (brain) and robustness to respiratory motion by comparing scans acquired in paced-breathing and free-breathing (kidney).

Results: In brain, all flow-based ASL techniques showed similar tSNR as pCASL, but only VSI-ASL showed similar sensitivity to perfusion changes. In kidney, all flow-based ASL techniques had comparable tSNR, although all lower than FAIR. In addition, VSI-ASL showed a sensitivity to B_1-inhomogeneity. All ASL techniques were relatively robust to respiratory motion.

Conclusion: In both brain and kidney, flow-based ASL techniques provide a planning-free and transit-time insensitive alternative to spatially selective ASL

techniques. VSI-ASL shows the most potential overall, showing similar performance as the golden standard pCASL in brain. However, in kidney, a reduction of B_1-sensitivity of VSI-ASL is necessary to match the performance of FAIR.

KEYWORDS

arterial spin labeling, brain, kidney, perfusion imaging, velocity selective ASL

1 | INTRODUCTION

Arterial spin labeling (ASL) is a non-invasive technique that can be applied in various organs to measure tissue perfusion. Traditionally, ASL uses spatially selective labeling of the blood to generate an endogenous tracer. In spatially selective labeling techniques, label is created proximal to the region of interest (ROI), after which a delay is inserted to allow the labeled blood to travel from the labeling location to the ROI. The currently recommended spatially selective ASL technique in the brain is pseudo-continuous ASL (pCASL).[1]

However, quantification issues can arise because of the time it takes for the labeled blood to flow from the labeling location to the ROI, (ie, transit time). For a subject with slow blood flow, transit times can become so long that the label signal has decayed before it reaches the ROI. Setting the transit times to match the delay times would lead to severe SNR loss. Whereas setting the delay times too short would lead to label still residing in the vascular compartment, making it impossible to discriminate between tissue that would be perfused later or tissue that would not be perfused at all, something that is often crucial for diagnosis or treatment selection.

Recently, a number of flow-based ASL techniques have been introduced where blood is labeled based on its flow velocity or acceleration instead of spatial location. Flow-based ASL techniques create label also within the ROI, making them less sensitive to transit delays.[2-5] Reduced sensitivity to transit delays is especially valuable in cases where blood flow is slow, for example, in elderly[6] patients with MoyaMoya disease[2,3,7] or in patients with renal artery stenosis.[8,9]

Moreover, flow-based ASL techniques do not require planning of a spatial labeling volume, making it easier and more time efficient to apply in practice. Planning of a spatial labeling volume can be especially challenging in the abdomen because of respiratory motion and (dynamic) field inhomogeneities.[1,10,11] In the kidneys, for example, ASL has been recognized as a promising tool to assess kidney function and identify pathology non-invasively,[8,12,13] however planning of the labeling slab for renal ASL can be time consuming and requirements for placement of the labeling slab can restrict the part of the kidney that is imaged.[14] Flow-based ASL can overcome these challenges, making it an interesting alternative to measure renal perfusion.

The first flow-based ASL technique, which is partly based on early suggestions by Norris and Schwarzbauer,[15] was proposed by Wong et al[16]: velocity-selective ASL (VSASL) uses motion-sensitized gradients (MSGs) to saturate blood magnetization above a certain cut-off velocity in the label condition, generating ASL signal based on the blood flow velocity. VSASL was followed by acceleration-selective ASL (AccASL),[17] where signal is created based on differences in blood flow acceleration (deceleration) instead of velocity. In 2015, multiple velocity-selective ASL (mm-VSASL)[18] was proposed, in which additional velocity selective saturation (VSS)-labeling modules are used to increase the amount of label created and therefore increase SNR. Velocity-selective inversion prepared ASL (VSI-ASL) was proposed. VSI-ASL uses a Fourier transform-based velocity-selective pulse train to generate label based on inversion of magnetization,[19] potentially doubling SNR compared to the saturation-based techniques. Whereas all of these techniques have their individual advantages and challenges, it is still unclear which technique is the most effective for perfusion measurements.

The aim of this study was to perform a direct comparison of these 4 flow-based techniques to the currently recommended spatially selective labeling techniques. This comparison was made both for brain, as well as, for kidney applications because the use of ASL is no longer restricted to just the brain. Moreover, flow-based ASL is hypothesized to behave differently in brain and kidney because of differences in flow-dynamics, B_0/B_1 field homogeneity, and organ motion.

In brain, flow-based ASL techniques were compared to pCASL, the golden standard in brain, based on temporal SNR (tSNR). In addition, sensitivity to identify perfusion changes was investigated using a visual task. In kidney the flow-based techniques were compared to the recommended methods in kidney, pCASL, and flow alternating inversion recovery (FAIR),[14] based on tSNR. In addition, robustness to respiratory motion was investigated by performing all scans both in paced- and free-breathing. Moreover, this is to the best of our knowledge, the first time that AccASL, mm-VSASL, and VSI-ASL are applied in kidney.

2 | THEORY

Figure 1 shows the sequence diagrams for all flow-based ASL techniques used in the current study. The VSASL sequence uses VSS-labeling and control modules. VSS modules

consist of 2 adiabatic hyperbolic secant inversion pulses and two 90° hard pulses.[16] Labeling is based on MSGs. The MSGs are only present in the label-module, so that under the assumption of a laminar flow profile, the magnetization of spins flowing above a cut-off velocity is saturated.[16] The last VSS-module in the sequence, right before the image acquisition, has MSGs in both label and control-condition. It acts as a crusher both for the labeled blood that has moved into the venous compartment and is accelerating, and for labeled blood that is still flowing above the cut-off velocity in the
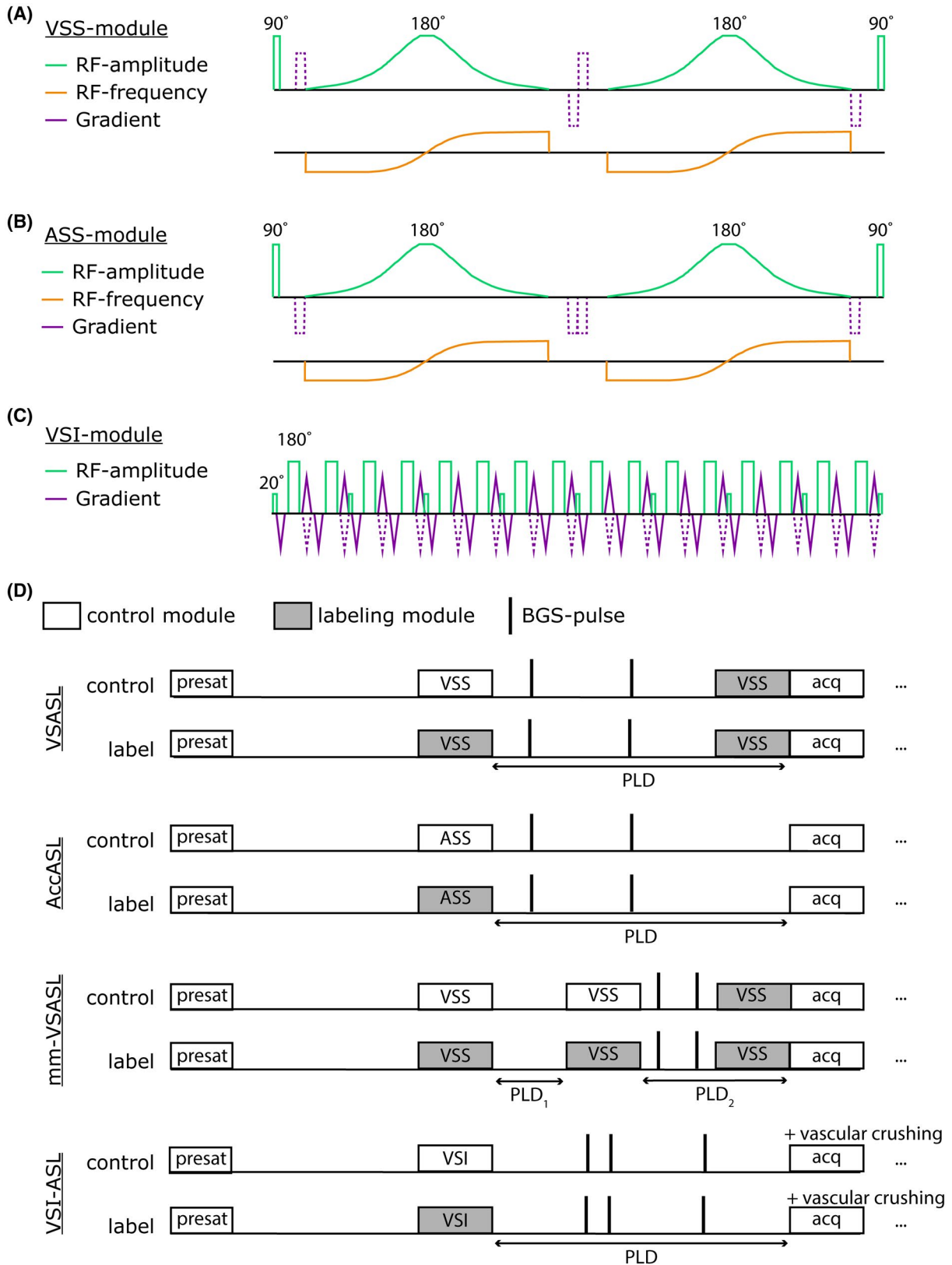
FIGURE 1 (A) A velocity selective saturation (VSS) label/control module is shown, including 2 90° hard RF-pulses, 2 adiabatic hyperbolic secant RF-pulses, and motion-sensitized gradients (MSG) in the label condition, as described in Wong et al.[16] These VSS modules are also used for mm-VSASL.[18] (B) An acceleration selective saturation (ASS) label/control module is shown, it consists of the same RF pulses as in the VSS module, only here the polarity of the MSG is only negative instead of alternating, as described in Schmid et al.[17] For AccASL, the MSG are only added in the label module. (C) A velocity selective inversion (VSI) label/control module is shown including 9 20° hard RF pulses and 16 phase-cycled 180° hard RF pulses and 8 sets of MSGs, as described in Qin and van Zijl.[19] In the label module the gradients have alternating polarity, whereas in the control module the polarity is solely negative. (D) Schematic sequence diagrams of the flow-based ASL-sequences; VSASL, AccASL, mm-VSASL, and VSI-ASL, incorporating the VSS, ASS, and VSI-modules shown in (A)–(C). Gray block represent the label modules, white blocks the control modules and the thick stripes represent the background suppression (BGS) pulses. A water suppression enhanced through T_1 (WET) module[21,22] is used as presaturation (presat) and multi-slice single-shot GE-EPI is used for acquiring images (acq). Image is not drawn to scale.

large vessels; moreover, it results in a predefined temporal width of the bolus of labeled spins as required for blood flow quantification. Mm-VSASL uses the same VSS modules, but has an additional label VSS module (Figure 1D).

AccASL uses acceleration-selective saturation (ASS) modules. The MSGs in the ASS modules are similar to ones in VSS modules, albeit played out with a negative polarity, leading to a phase-dependence on spin acceleration (or deceleration) instead of velocity (Figure 1B).[17] By subtracting label from control signal, signal is generated only from the spins with an acceleration (or deceleration) above the cut-off.[17,20] AccASL has not been implemented yet using a second labeling module.[17] This makes quantification of the AccASL signal currently not possible, because the temporal width of the bolus would be unknown.

VSI-ASL is based on a slightly different principle. VSI-modules incorporate a Fourier transform-based velocity-selective pulse train in the form of nine 20° hard pulses in combination with 16 phase-cycled 180° hard pulses to achieve inversion of the magnetization in small steps (Figure 1C). Labeling of spins above the cut-off velocity is achieved by using bipolar MSGs in the label condition and negative polarity gradients in the velocity-compensated control condition (Figure 1D).[19] This leads to an inverted magnetization for spins flowing below the cut-off velocity during the label condition and an inverted magnetization of all spins during the control condition.[19] In VSASL and mm-VSASL, a VSS module right before image acquisition is used to crush the venous and vascular contribution to the ASL signal and to enable quantification. In VSI-ASL, vascular crushing was enabled for the same purpose. Here, the crushing of spins above the cut-off velocity is performed during the acquisition instead of right before. No major differences between the 2 approaches were found previously.[16]

3 | METHODS

3.1 | Data acquisition

All flow-based ASL techniques (VSASL, AccASL, mm-VS-ASL, and VSI-ASL) were acquired in the brain and kidneys

and compared to the reference ASL technique(s) in the respective anatomies.

Data were acquired on 3T Philips (Philips Healthcare, Best, The Netherlands) scanners and this study was performed with approval of the local institutional review board. Written informed consent was obtained from each subject before inclusion. Brain and kidney scans were acquired in separate scan sessions and separate subjects.

3.1.1 | Brain

For brain, pCASL is currently the standardized ASL technique,[1] and was therefore used as reference technique. The brain scan sessions consisted of 2 conditions; all ASL techniques were first acquired while the subject was watching a cartoon and a second time with eyes closed. Within each condition, the order of the ASL techniques was randomized. The visual stimulus is expected to induce a perfusion increase in the visual cortex. By subtracting the perfusion signal during rest and visual stimulus, the sensitivity to detect small increases in perfusion can be measured for each ASL technique.

Five healthy subjects (24–60 years, 2 male and 3 female) were included. Images were acquired using a 32-channel head coil and a multi-slice single-shot gradient-echo EPI acquisition. Image acquisition was planned in oblique transversal orientation, parallel to the corpus callosum in sagittal view. Scan parameters for VSASL, AccASL, mm-VSASL, and VSI-ASL were chosen based on previous research[16-19] (Table 1). The post-labeling delays (PLDs) of flow-based ASL techniques are usually shorter than those of spatially selective techniques, because labeling takes place in or close to the microvascular bed. The PLD of flow-based ASL can, however, not be chosen too small, because the PLD also control the bolus duration: only spins that have decelerated below the cut-off velocity during the PLD will contribute to the perfusion signal. mm-VSASL, therefore, requires a slightly longer total PLD to also allow the spins saturated by the second module to decelerate. For the current study the PLD-settings were taken from the quoted literature.

The duration of the VSASL-, AccASL-, and mm-VSASL labeling modules were set to 50 ms, to allow enough time for an adiabatic angle of 1500° for the hyperbolic

TABLE 1 Scan parameters used brain and kidney

Scan parameter	VSASL[16]	AccASL[17]	mm-VSASL[18]	VSI-ASL[19]	pCASL[1]	FAIR[24]
Brain						
Voxel size (mm)	$3 \times 3 \times 7$	$3 \times 3 \times 7$	$3 \times 3 \times 7$	$3 \times 3 \times 7$	$3 \times 3 \times 7$	–
No. slices	17	17	17	17	17	–
Recovery after presaturation (ms)	2000	2000	2000	2000	–	–
TR (ms)	4260	4260	4610	4160	4170	–
No. repetitions	28	28	28	28	28	–
Total scan duration (min:s)	4:07	4:07	4:27	4:01	4:01	–
Post-labeling delay (ms)	1600	1600	[1150,820]	1500	1800	–
Background suppression (ms)	[50,1150]	[50,1150]	[20,620]	[560,580,1140]	[112,1350]	–
Cut-off velocity or acceleration	2 cm/s	1.8 m/s^2	2 cm/s	2.8 cm/s	–	–
Duration labeling module (ms)	50	50	50	48	1800	–
No. labeling modules	1	1	2	1	1	–
VS-crushing during or before acquisition (cm/s)	2	–	2	3	–	–
Kidney (PB/FB)						
Voxel size (mm)	$3 \times 3 \times 6$	$3 \times 3 \times 6$	$3 \times 3 \times 6$	$3 \times 3 \times 6$	$3 \times 3 \times 6$	$3 \times 3 \times 6$
No. slices	5	5	5	5	5	5
Recovery after presaturation (ms)	4908/3000	4908/3000	4130/3000	4908/3000	–	–
TR (ms)	6500/4600	6500/4600	6500/5380	6500/4630	6500/6340	6500/4750
No. repetitions	21	21	21	21	21	21
Total scan duration (min)	4:46/3:22	4:46/3:22	4:46/3:56	4:46/3:23	4:46/4:39	4:46/3:29
Post-labeling delay	1200	1200	[1150,820]	1200	1500	1400
Background suppression (ms)	[100,940]/ [100,925]	[100,940]/ [100,925]	[20,660]/ [20,650]	[350,650,1080]/ [350,650,1070]	[1520,2530]/ [1520,2530]	[500,1020]/ [500,1020]
Cut-off velocity or acceleration	5 cm/s	1.4 m/s^2	5 cm/s	5 cm/s	–	–
Duration labeling module (ms)	50	50	50	48	1800	15
No. labeling modules	1	1	2	1	1	1
VS-crushing during or before acquisition (cm/s)	5	–	5	5	–	–
Q2TIPS[25]: 5 120-mm saturation slabs evenly spaced	–	–	–	–	–	1200−1300 ms

For the bottom (kidney) panel: settings that differ between the paced- and free-breathing scans are indicated as (paced-breathing)/(free-breathing). For all scans, hyperbolic secant pulses were used as background suppression pulses.

Abbreviations: VSASL, velocity selective arterial spin labeling; AccASL, acceleration-selective ASL; mm-VSASL, multiple velocity selective arterial spin labeling; VSI-ASL, velocity selective inversion; pCASL, pseudo-continuous ASL; FAIR, flow alternating inversion recovery.

secant refocusing pulses. Gradient orientation for VSASL, AccASL, and mm-VSASL was in the slice-direction (ie, feet–head direction). The number of repetitions was kept constant between all ASL scans. Background suppression (BGS) using hyperbolic secant pulses was applied in all sequences, resulting in 85%–90% suppression of tissue signal for the first slice. All ASL techniques except for VSI-ASL used 2 BGS pulses. VSI-ASL used 3 BGS pulses to compensate the static tissue inversion performed by the VSI-ASL modules. This makes sure that the static tissue signal is positive on image acquisition. The exact BGS pulse timings are reported in Table 1; defined from the end of

the VSS-labeling module, and in case of mm-VSASL, the end of the second VSS-labeling module. Water suppression enhanced through T_1 (WET) presaturation[21,22] was used to avoid spin history effects (Figure 1D), and the TR was adjusted to accommodate a 2-s recovery of the WET presaturation for all flow-based ASL techniques. In case of pCASL, the WET presaturation was placed right before labeling and therefore did not require a TR-adjustment to accommodate regrowth of the magnetization.

A sagittal and coronal phase-contrast enhanced MRA localizer was used to aid planning of the pCASL labeling slab, using an encoding velocity of 40 cm/s and a total scan

duration of 54 s. The pCASL labeling slab was planned perpendicular on the dorsal part of the vertebral arteries at the height of C1/C2.

An M_0 scan, for calibration of the ASL signal, was acquired using the same acquisition as the ASL scans with ASL labeling turned off and using a TR of 10 s. A 3D T_1-weighted scan, for gray matter segmentation, was acquired using a multi-shot 3D-TFE acquisition, with a TR/TE of 9.7/4.6 ms, and acquisition voxel size of 1.2/1.2/1.2 mm, resulting in a total scan duration of 5 min.

3.1.2 | Kidney

For kidney, both pCASL and FAIR are recommended,[14] and therefore, both were used as reference techniques. The kidney scan sessions consisted of 2 conditions; all ASL techniques were first acquired in paced breathing and a second time in free breathing. Within each condition, the order of the ASL techniques was randomized. In the paced-breathing condition, subjects were asked to synchronize their breathing with the image acquisition (ie, to perform a shallow breath in and out in between the acquisitions and to hold their breath briefly on exhalation during the acquisition). The researcher provided coaching for the first couple of breaths via the intercom. Subject cooperation was checked using a respiratory bellow for both breathing conditions. Robustness to breathing strategy was investigated by comparing the tSNR per unit time during paced- and free-breathing.

Six healthy subjects (23–30 years, 3 male and 3 female) were included. Images were acquired using a 28-element phased-array body coil and a multi-slice single-shot gradient-echo EPI acquisition. Image acquisition was planned in coronal–oblique orientation, parallel to the muscles anterior to the kidney, to minimize through-slice motion. Optimal scan parameters for renal imaging were not known for all flow-based ASL techniques, so they were chosen partly based on previous research[5,23,24] and partly on preliminary experiments (Table 1). The durations of the VSS- and ASS-labeling modules were set to 50 ms, and gradient orientation to the slice direction, that is, anterior–posterior (AP) direction, to minimize effects of respiratory motion on labeling.[5] FAIR was implemented as described in Harteveld et al,[24] including Q2TIPS,[25] which was placed anterior to the imaging acquisition with a 10-mm gap (Table 1).

For all ASL scans, the number of repetitions was kept constant. BGS using hyperbolic secant pulses were applied in all sequences, resulting in 85%–90% suppression of tissue signal for the first slice. WET presaturation[21,22] was used to avoid spin history effects (Figure 1D), and saturation slabs were placed superior and inferior to the imaging volume to minimize fold-in artefacts. RF shimming was performed on a volume shim box that covered the image acquisition volume

with an additional 10 mm on each side in the AP direction. B_0 shim was set to automatic. A TR of 6500 ms was used for the paced-breathing scans to keep the breathing rhythm as natural as possible. For the free-breathing scans, the TR was adjusted to accommodate a 3-s recovery of the saturation slabs and WET presaturation.

The flow-based ASL techniques did not require additional planning of a labeling slab. For FAIR, the selective labeling slab, and therefore, the imaging volume, was planned such that it excluded the aorta to ensure labeling of the aorta. The pCASL labeling slab was planned perpendicular to the aorta. Care was taken to not place the pCASL labeling slab too inferiorly to minimize the chance of the kidneys moving into the labeling slab during breathing and also not place it too superiorly to minimize negative effects on labeling efficiency from field inhomogeneities at the air–tissue interface of the lungs.

In addition to the ASL scans, an M_0 and a T_1-map was acquired with the same planning as the ASL acquisition. The M_0 scan was acquired in paced breathing for calibration of the ASL signal, using the same acquisition as the ASL scans, with ASL-labeling turned off and using a TR of 6500 ms. The T_1-map was acquired for segmentation of kidney cortex and medulla. It was acquired using a cycled multi-slice inversion–recovery sequence[26] with 11 inversion times ranging between 42 ms and 2030 ms, and a multi-slice single-shot EPI acquisition, resulting in total scan duration of 1 min 18.

A B_1-map was acquired in 2 subjects, and in 1 of these subjects, an additional VSI-ASL scan was acquired without BGS using 10 repetitions. These additional scans were acquired to investigate the origin of an artefact of VSI-ASL in the kidney that became apparent during scanning. The B_1 map was acquired using a dual-TR method[27] with a TR of 30 ms and 150 ms, and a gradient spoil factor of 20. The B_1 map received the same planning as the ASL acquisition (see the Supporting Information S1, and Supporting Information Figures S1 and S2 for these results and further simulations on the VSI-ASL artefact).

3.2 | Post-processing

Using SPM12,[28] the brain ASL scans were first realigned and co-registered to the T_1-weighted scan and later transformed to MNI space and smoothed (kernel width = 8 × 8 × 8 mm). Using Mevislab[29] (MeVis Medical Solutions AG, Fraunhofer MEVIS, Bremen, Germany), all kidney scans were co-registered to each other using a groupwise image registration method,[30] separately for left and right kidney.

The ASL subtraction images (ΔM_i) were normalized by M_0 and averaged over all n repetitions to obtain a perfusion-weighted signal (PWS) map and enable inter-subject comparison.

$$\text{PWS} [\%] = \frac{1}{n} \sum_{i=1}^{n} \frac{\Delta M_i}{M_0}. \tag{1}$$

Voxel-wise tSNR was calculated by dividing the average ASL signal over time ($\mu_{\Delta M,voxel}$) by the SD of the ASL signal over time per voxel ($\sigma_{\Delta M,voxel}$).

$$\text{tSNR}_{voxel} = \frac{\mu_{\Delta M,voxel}}{\sigma_{\Delta M,voxel}}. \tag{2}$$

Whole brain masks were created by thresholding the M_0 image, and whole kidney masks were created by manually drawing kidney contours on the M_0 image. These masks were used for visualization. For the tSNR graphs, gray matter masks were generated based on the T_1-weighted brain scans using the SPM12 Toolbox,[28] voxels with >70% gray matter included in the mask. Cortex, medulla, and high intense fluid masks were generated based on the kidney T_1 map using an intensity histogram to manually threshold the image. This study showed artefacts in the VSI-ASL kidney images in some subjects with the severity of the artefact varying greatly between subjects. To enable a fair comparison between results, individual artefact masks were manually drawn on the VSI-ASL images and the voxels inside the artefact mask excluded for the tSNR analysis of VSI-ASL. Additional scans and simulations on the VSI-ASL artefact in kidney can be found in the Supporting Information S1, and Supporting Information Figures S1 and S2.

3.2.1 | Statistical analysis

For both the brain and kidney data set, a repeated-measures analysis of variance (ANOVA) in combination with a Tukey post hoc test was applied to test whether there are significant differences in terms of tSNR between the different ASL techniques, using $P = 0.05$. Data are reported as mean $\pm$ SD.

To study the effect of visual stimulation on brain PWS, a voxel-wise repeated-measures ANOVA was performed to test whether the PWS values acquired during rest and during visual stimulation conditions significantly differed from each other. All PWS repetitions (without averaging) of all subjects were used as input, setting subjects as between-group factor. Analysis was performed after transforming the PWS maps to MNI space. A Bonferroni correction was applied to correct for multiple testing, resulting in $P = 2.6\text{e}{-7}$.

The effect of breathing strategy was evaluated using tSNR per unit time, to compensate for the shorter TR of the free-breathing scans. The mean tSNR-values in cortex were divided by the square root of the time it takes to acquire 1 label–control pair.

$$\text{tSNR}_{per\ unit\ time} \left[s^{-1/2} \right] = \frac{tSNR}{\sqrt{2 * TR}}. \tag{3}$$

A paired Student's t-test was used to test whether the tSNR per unit time differed significantly between scans acquired in paced- and free-breathing, using $P = 0.05$.

4 | RESULTS

4.1 | Brain

PWS and tSNR maps of a representative subject are shown in Figure 2. Comparison of PWS maps between ASL techniques showed that VSI-ASL had a similar spatial pattern as the reference sequence (ie, pCASL; Mm-VSASL showed very high signal in CSF-rich areas). VSASL and AccASL also both showed higher signal in areas with CSF, although to a lesser degree than mm-VSASL.

Figure 3 shows the distribution over subjects of the mean tSNR in gray matter, for all ASL techniques. VSASL, AccASL, mm-VSASL, VSI-ASL, and pCASL all have similar mean tSNR in gray matter without significant difference ($P > .05$), although the SD of the tSNR over subjects is larger for VSASL and mm-VSASL (tSNR mean $\pm$ SD VSASL = 1.07 $\pm$ 0.52, AccASL = 1.27 $\pm$ 0.24, mm-VSASL = 1.36 $\pm$ 0.55, VSI-ASL = 1.18 $\pm$ 0.12, and pCASL = 1.10 $\pm$ 0.09).

Next, the ability to measure small increases in perfusion on visual stimulation was compared between all ASL techniques. VSI-ASL and pCASL detected the visual cortex most robustly, as evidenced by the highest number of voxels in the visual cortex that showed statistically significant increased PWS (Figure 4). VSASL, AccASL, and mm-VSASL showed less power, less voxels showed significant increases in perfusion and P-values were higher.

4.2 | Kidney

One subject was excluded because of excessive through-plane motion during the scans, leaving 5 subjects available for analysis.

Figure 5A shows representative PWS maps from 1 subject. The flow-based ASL techniques all showed clear corticomedullary contrast with spatially homogeneous signal in the cortex region, similar to the 2 reference techniques (ie, FAIR and pCASL). Between the flow-based techniques, VSI-ASL and AccASL show a slightly higher PWS compared to the rest. In general, flow-based techniques had a similar PWS-intensity as pCASL, but clearly lower than FAIR. The flow-based ASL techniques displayed small abnormalities at locations that are part of the collecting system, indicated by the green arrows in Figure 5A. In addition, negative signal was sometimes observed in the medulla, especially for VSI-ASL.

FIGURE 2 (A) Brain perfusion-weighted signal (PWS) maps of a representative subject. As expected, mm-VSASL and to a lesser extent VSASL and AccASL showed some T_2- and/or diffusion-weighting,[2-4] illustrated by the high signal in areas rich in CSF (B) Temporal SNR (tSNR) maps of a representative subject
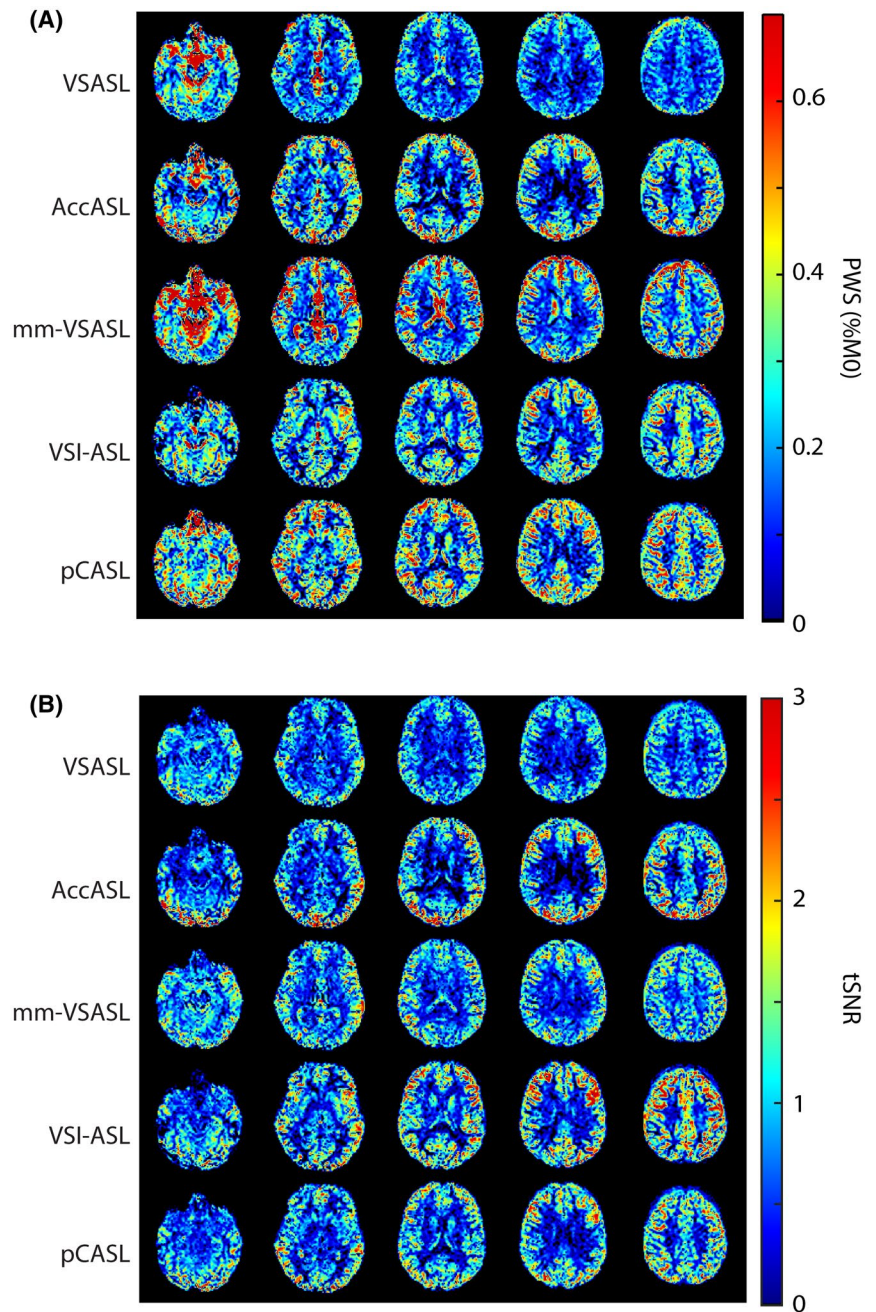
A similar pattern was observed on group level in the tSNR graphs of Figure 5B; all flow-based ASL techniques showed a similar tSNR as pCASL, but significantly lower than FAIR in cortex (tSNR mean ± SD VSASL = 1.59 ± 0.21, AccASL = 1.54 ± 0.41, mm-VSASL = 1.37 ± 0.34, VSI-ASL = 1.62 ± 0.36, pCASL = 1.79 ± 0.56, and FAIR = 4.61 ± 0.71) ($P < .05$), as well as medulla (VSASL = 0.43 ± 0.11, AccASL = 0.66 ± 0.09, mm-VSASL = 0.50 ± 0.06, VSI-ASL = 0.17 ± 0.14, pCASL = 0.46 ± 0.15, and FAIR = 1.42 ± 0.55) ($P < .05$). The tSNR in the medulla is notably lower than in the cortex. Note that in the tSNR graphs in Figure 5B voxels that are part of the VSI-ASL artefact mask were not taken into account for the VSI-ASL images

(see Supporting Information Figure S3 for the tSNR graphs including all voxels).

Next, sensitivity of the flow-based ASL scans to breathing strategy was investigated (Figure 6). VSASL and AccASL both showed a reduction of ~14% in mean tSNR per unit time for the free-breathing condition, whereas hardly any reduction of tSNR per unit time was observed for mm-VSASL and VSI-ASL (respectively <0.01% and −0.03%). However, none of the flow-based ASL techniques showed a statistically significant decrease in tSNR per unit time. Only FAIR, showed a statistically significant lower tSNR per unit time for the free-breathing condition ($P < .05$), although the difference was small (~14.2%) (Figure 6).
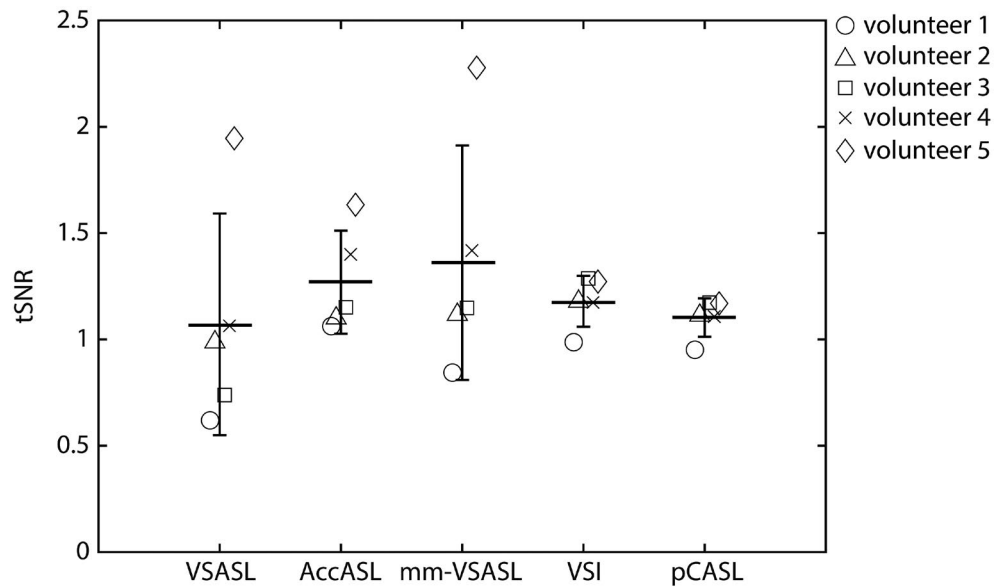
FIGURE 3 Distribution of mean temporal SNR (tSNR) in gray matter over subjects, for all ASL techniques. Middle bar represents the mean tSNR value over all subjects, and the vertical bars represents the SD
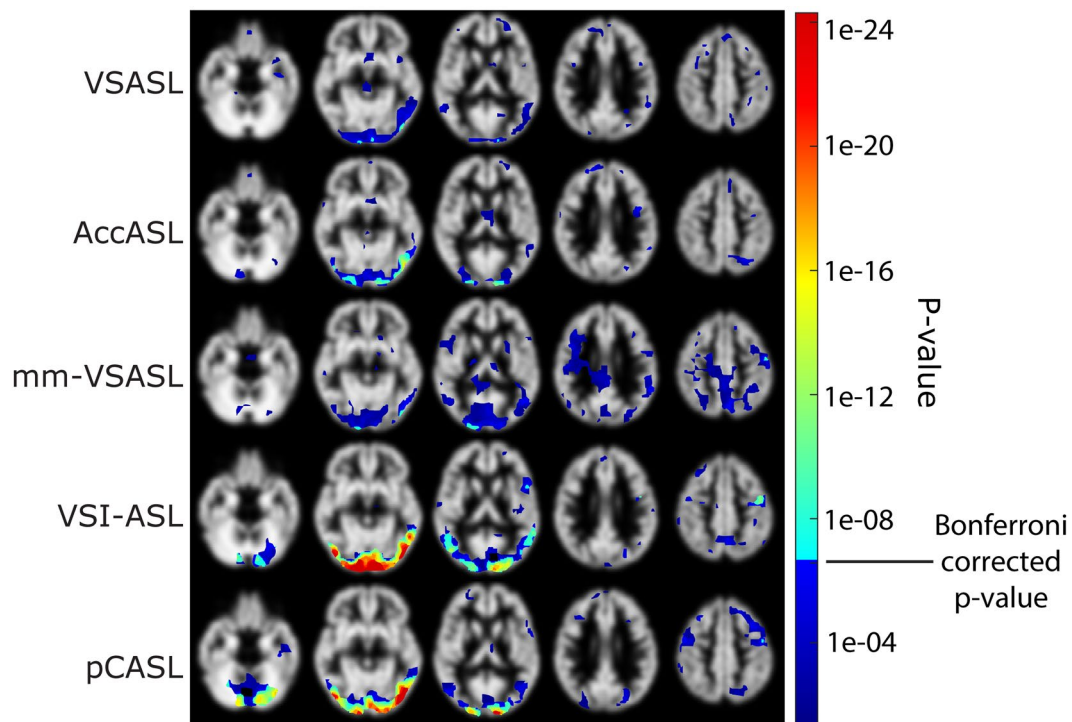

FIGURE 4 Visual activation maps of the brain averaged over all subjects, showing the voxels with a higher perfusion-weighted signal (PWS) value during visual stimulus (watching cartoon) compared to rest (eyes closed). A Bonferroni correction was applied to correct for multiple testing, resulting in a significance level of $P = 2.6e{-}7$. Color indicates the P-value. Results are overlain on a gray matter segmentation. Five brain slices are shown

5 | DISCUSSION AND CONCLUSIONS

This study has shown that flow-based ASL techniques are feasible in both the brain and kidneys at 3T, enabling

planning-free ASL measurements with intrinsically reduced sensitivity to transit time artefacts. In brain, results showed that all flow-based ASL techniques had comparable robustness of the signal (tSNR) to the reference pCASL. However, only VSI-ASL showed similar sensitivity as
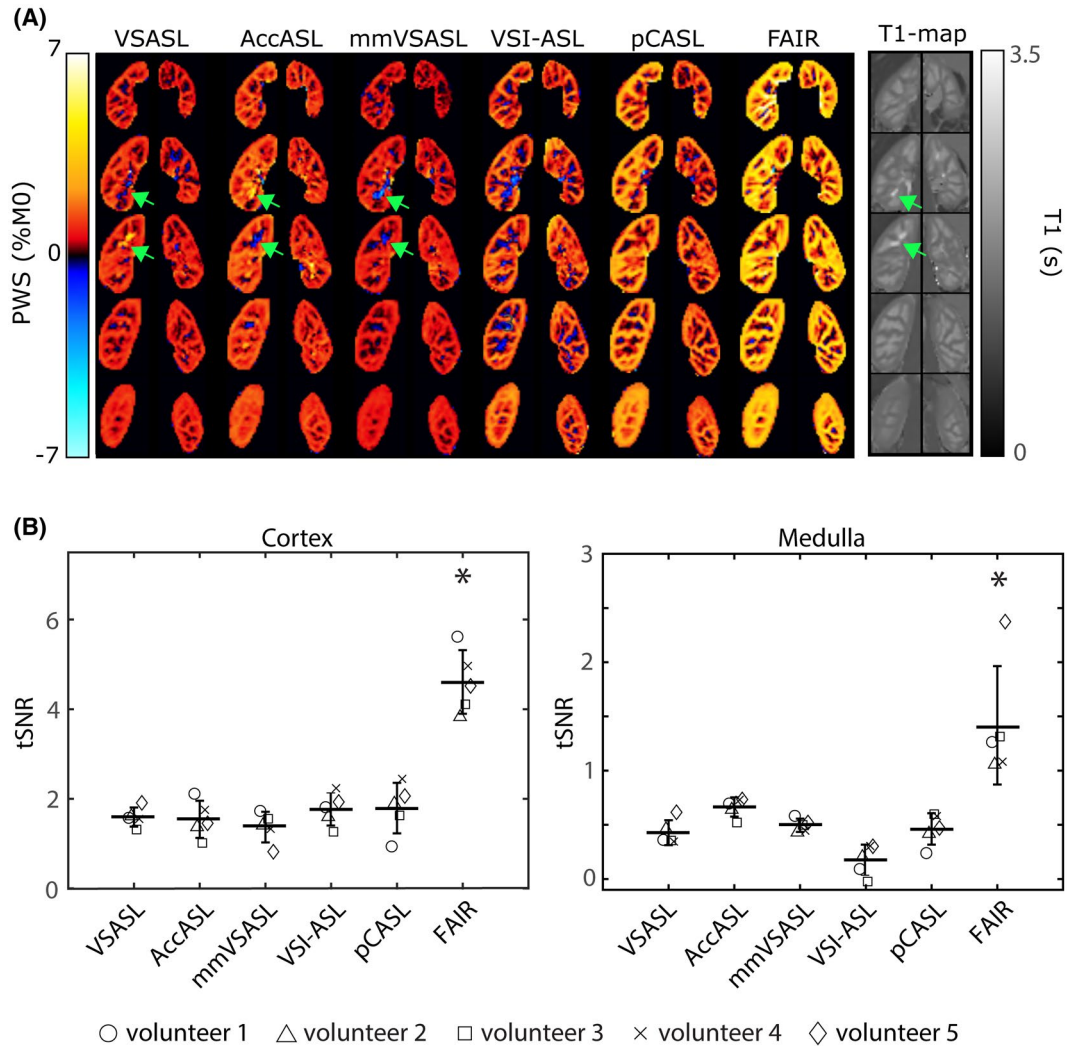
FIGURE 5 (A) Kidney perfusion-weighted signal (PWS) maps of a representative subject acquired during paced breathing. The green arrows indicate locations that are part of the collecting system, where the flow-based ASL techniques displayed either intense positive or negative signal. (B) Distributions of mean temporal SNR (tSNR) in cortex and medulla over all subjects, for all ASL techniques. Flow alternating inversion recovery (FAIR) had a statistically significant higher tSNR than all other ASL techniques indicated by the asterisk ($P < .05$), for both cortex and medulla. Note that for VSI-ASL the voxels that were part of the artefact mask were not taken into account

pCASL for picking up small increases in brain perfusion. In the kidneys, all flow-based ASL techniques showed similar PWS and good corticomedullary contrast. However, compared to the reference technique FAIR, all flow-based ASL techniques had significantly lower tSNR. The flow-based ASL techniques proved to be robust to respiratory motion when using image registration, enabling free-breathing acquisition.

In brain, a comparable tSNR was found for all flow-based ASL techniques (VSASL, AccASL, mm-VSASL, and VSI-ASL) and pCASL. VSASL, mm-VSASL, and AccASL showed a higher variability of tSNR over subjects than VSI and pCASL, although this could mainly be attributed to a single subject. Further inspection showed that this subject had a deviating CSF system compared to the other subjects (see Supporting Information Figure S4A). Possibly,

partial volume effects in combination with the inherent diffusion-weighting of VSASL, AccASL, and mm-VSASL can explain the increased tSNR in this subject compared to the others. See Supporting Information Figure S4B for a representation of the ASL-data in the gray matter segmentation.

Previously, in comparison, a significantly lower tSNR for VSASL was found compared to AccASL and pCASL.[17] Discrepancy in the results could be because of the use of a lower flip angle of the adiabatic refocusing pulses in Schmid et al[17] compared to the current study. In the current study, adiabatic refocusing pulses were used with a higher flip angle and with a slower rotation of the effective B_1-field that better satisfied the adiabatic condition. This resulted in a 50-ms VSS-labeling module instead of 30-ms. The gains from improved adiabaticity outweighed the losses from increased T_2 decay as a result of a longer duration.
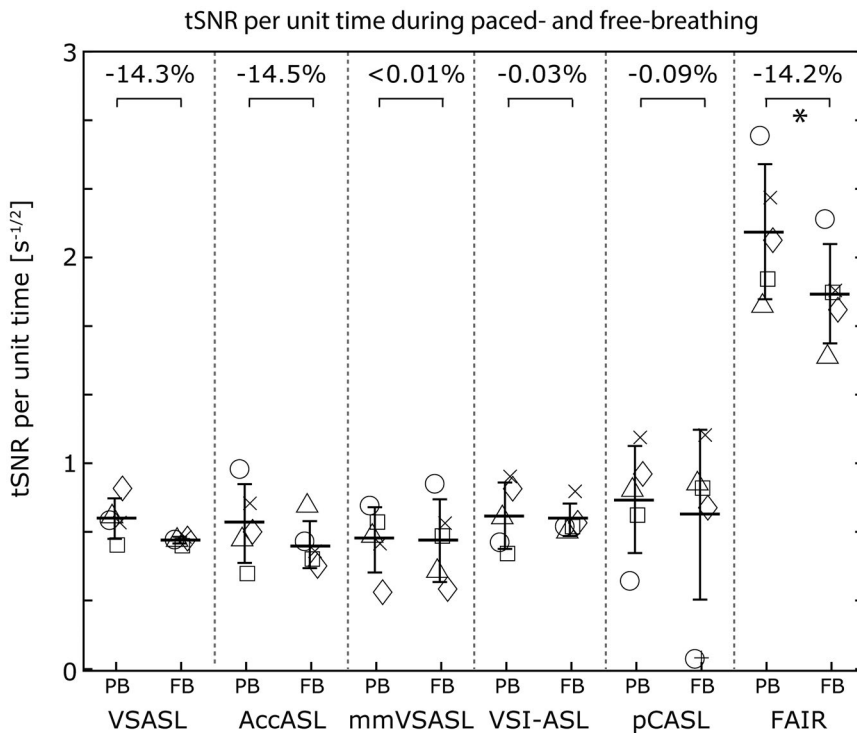
FIGURE 6 Temporal SNR (tSNR) per unit time for all subjects in the kidney cortex, during paced- (PB) and free-breathing (FB). At the top the mean paired difference between PB and FB tSNR per unit time is given in percentages. Only FAIR has a statistically significant lower tSNR per unit time during free-breathing, but this difference is small (-12.2%)

Guo and Wong[18] reported that ASL-signal of gray matter (treated as a direct indicator of spatial SNR) of mm-VSASL was significantly higher than VSASL and was similar to that of pCASL. In the current study, tSNR was used to compare the different techniques instead of spatial SNR, since tSNR also takes signal robustness into account. A similar tSNR for VSASL, mm-VSASL, and pCASL was found. Although when solely looking at the ASL signal, mm-VSASL did show a higher value than VSASL and pCASL, albeit with a larger SD over time (see Supporting Information Figure S5). In addition, Guo and Wong[18] used a B_1-insensitive rotation (BIR)-8 implementation of VSASL, which has been shown to be more resistant to eddy currents and B_1-inhomogeneities,[31,32] instead of the VSASL implementation shown in Figure 1A. Qin and van Zijl[19] reported a similar tSNR between VSI-ASL and pCASL and comparable values were measured in the current study.

Results in the brain showed that all flow-based ASL techniques have similar tSNR to pCASL. However, tSNR provides information on ASL signal stability over time, but does not provide evidence on the sensitivity of the technique to detect small changes in cerebral blood flow (CBF). To test this, a mild visual stimulus was given. From the flow-based ASL techniques, VSI-ASL showed a similar sensitivity to pick up changes in perfusion as pCASL, confirming a recent perfusion-weighted functional MRI study,[33] whereas VSASL, AccASL, and mm-VSASL showed less power. The reason why VSASL, AccASL, and mm-VSASL showed lower sensitivity to detect CBF-changes compared to VSI, even though they have similar tSNR, is probably because of the fact that they are more prone to subtraction errors because of, for example, diffusion. These errors contribute to a high tSNR, but do not contribute to the visual activation map. This, together with previous findings that VSI-ASL produces similar CBF-maps as pCASL,[19] implies that VSI-ASL is the most promising flow-based ASL technique for brain applications.

Diffusion-weighting of the VSASL-, AccASL-, and especially mm-VSASL signal, visible as high signal in CSF-related areas, has also been observed in previous studies.[16-18] Diffusion sensitivity of VSASL, AccASL, and mm-VSASL is caused by the fact that the VSS- and ASS-labeling module contains motion-sensitizing gradients and the control module does not. The mm-VSASL signal is especially affected, possibly because of the additional VSS-labeling module. A diffusion correction should be applied when using VSASL or mm-VSASL for quantification,[5] to prevent overestimation of the CBF. AccASL cannot be quantified at the moment, because the bolus duration is unknown.[17]

In kidneys, tSNR was comparable for all flow-based ASL techniques and pCASL. However, compared to FAIR, all flow-based techniques had a significantly lower tSNR in both cortex as well as medulla. VSASL was previously compared to pCASL at 1.5T, and a lower whole kidney tSNR for VSASL compared to pCASL was reported.[5] The discrepancy in results is likely caused by a higher B_0-inhomogeneity at 3T reducing the labeling efficiency of pCASL, thereby reducing the benefits of pCASL with respect to VSASL.

The observed lower tSNR for flow-based ASL techniques compared to FAIR could be caused by a lower labeling efficiency of the flow-based ASL techniques, possibly because of a higher sensitivity to field inhomogeneity or because of

the dependence on flow direction. Labeling by flow-based ASL is only sensitive to flow in a single direction, as determined by the orientation of the labeling gradients. Labeling directions were chosen based on the primary directions of flow and also, orthogonal to the direction of respiratory movement to mitigate possible bulk motion artefact, as has been observed previously.[5] Besides this, previous studies in both brain[16] and kidney[5] have found little dependence of the VSASL signal on the labeling-direction for a cut-off velocity of <4 cm/s and 5 cm/s in brain and kidney, respectively. More research is necessary to be able to draw final conclusions the precise reason why FAIR performs better than flow-based ASL in the kidneys.

Although it was not the subject of the current study, the tSNR difference between the 2 standard techniques in kidney ASL, FAIR, and pCASL, is noteworthy. We found a 3× higher tSNR for FAIR compared to pCASL. Similar differences were found in a previous study,[24] where a detailed discussion is provided on the reasons why pCASL performed worse than FAIR in kidney at 3T, given that the opposite is true for the brain. Advantages of pCASL in brain include labeling closer to the imaging region and having a longer temporal bolus. However, these do not hold for kidneys. In the kidneys, the labeling plane of pCASL was planned 15 cm above the kidneys and the temporal bolus of FAIR is increased because blood is labeled in most of the torso. This provides a possible explanation of the higher tSNR of FAIR that was found in this study. However, it is important to keep in mind that there are also downsides to using FAIR in kidneys. Coronal imaging is recommended for renal applications, so that through-slice motion because of respiration is minimized and blood is labeled closer to the kidney in the renal arteries. However, using coronal imaging comes with its own complications. First of all, it is cumbersome to plan the selective labeling slab, because the aorta needs to be excluded. Second, coronal FAIR does not always allow full organ coverage, because of the constraint of excluding the aorta from the imaging region (between 54%–80% of the kidney could be covered in the current study). This is why it is often used as a single-slice technique.[14] Flow-based ASL techniques can provide a time-efficient alternative that guarantees whole organ coverage, albeit with lower tSNR.

In the current study a generally lower tSNR was found for kidney medulla compared to cortex, which was expected because the medulla has a lower perfusion than the cortex, only ~10% of renal blood flow reaches the medulla.[13,34] However, the finding that FAIR has a significantly higher tSNR in medulla was not necessarily expected. Because of the longer transit times of medulla,[24] one would expect that flow-based ASL techniques are better suited to measure medullary perfusion than the spatially selective ASL techniques. However, it is likely that the cut-off velocity was still too high to label directly in the medulla. Unfortunately, the cut-off velocity

cannot be chosen lower than 5 cm/s without risking respiratory motion artefacts.[5] Nevertheless, results did show that the relative performance of flow-based ASL in the medulla was improved compared to that in the cortex.

Flow-based ASL in kidney also showed some artefacts in locations related to urine. This can be explained by the fact that although the ASL-module was played out, the collecting system will have high signal compared to kidney tissue, because of the short T_1 of urine. Small motion or diffusion-weighting of the urine signal will subsequently generate subtraction artefacts that can either be positive or negative.

Results showed that respiratory motion only plays a small role for flow-based ASL in kidney when using image registration. A reduction in tSNR per unit time was observed during free-breathing for all flow-based ASL techniques, although it was not statistically significant for any of the techniques. Indicating that up to a certain point, the shorter TR of free-breathing scans compensate for the reduction in tSNR by facilitating acquisition of more repetitions. This is in line with the paper by Robson et al,[35] where they conclude that rejection because of motion artifacts during free-breathing acquisition is offset by being able to acquire more data in the same scan time. In contrast to Robson et al, in the current study a fast field echo-EPI acquisition was used and no repetitions needed to be rejected because of motion.

In practice, the limited reduction in tSNR per unit time is outweighed by the great improvement to patient comfort and practicability. An additional benefit of acquiring scans in free-breathing is that images will be acquired during every respiratory state, which gives a more representative sampling of the hemodynamic state.

This study has shown that the performance of flow-based ASL techniques in kidney is still less convincing than in brain. In kidney, all flow-based ASL techniques had a significantly lower tSNR than FAIR, whereas in brain flow-based VSI-ASL provides comparable performance to pCASL.

Given the results in brain, VSI-ASL holds the most promise to improve the performance of flow-based ASL in kidney. However, VSI-ASL in kidney showed severe subtraction artefacts in some individuals. Additional scans and simulations were performed to investigate the underlying cause (see Supporting Information S1 and Supporting Information Figures S1 and S2). Results indicate that the combination of suboptimal inversion of the static tissue by VSI-ASL and of the BGS pulses is likely the cause of the negative tissue signal that was observed in low-B_1 areas. The precise underlying cause and possible solution for the VSI-ASL artefacts observed in kidney warrants further research.

This study has some limitations. First of all, during the paced-breathing condition subjects were asked to shortly hold their breath during the image acquisition, but not necessarily during labeling. However, effects are expected to be small because a cut-off velocity (5 cm/s) was chosen to

prevent subtraction artefacts because of respiratory motion, and our results indeed did not show the typical high intensity subtraction artefacts as described by Bones et al.[5] In addition, VSASL- and AccASL-labeling have been shown to depend on the cardiac cycle.[36] Effects are expected to average out when using a sufficient number of averages, but will still lower tSNR-values.

Second, as mentioned before, the current study used a VSASL implementation as described by Wong et al[16] instead of the BIR-8 implementation of VSASL,[31,32] which has been shown to reduce eddy current effects as well as sensitivity to B_1. However, when using a PLD of 1500 ms and a cut-off velocity of 2 cm/s, similar CBF-maps were produced for both VSASL implementations,[32] so this is not expected to have had a major effect on our data.

Third, balanced pCASL was used as 1 of the reference techniques. Recently, optimized unbalanced implementations of renal pCASL were presented in a limited number of subjects, to reduce sensitivity to B_0-inhomogeneities.[11,37] Using 1 of the optimized implementations could improve the performance of pCASL as reported in this study. However, a separate shimming area at the labeling location is used in our pCASL implementation, which will reduce off-resonance artefacts when using balanced pCASL.

In addition, the PLDs used in renal mm-VSASL as taken from literature, were optimized for brain applications. Possibly the renal PWS of mm-VSASL could be improved by optimizing the PLDs specifically for kidneys.

Last, perfusion data in this study were not quantified. The main focus of the study was to provide a comparison on the performance of techniques without too much emphasis on differences in tracer kinetics and modelling assumptions that would result in technique-specific scaling factors. By dividing by M_0 inter-subject differences in scanner settings are accounted for, and without an additional subject-specific T_1 and labeling efficiency measurement, quantification would only add a technique-specific scaling factor. Quantitative comparison would especially be interesting when a gold standard reference, like PET, would be available.

In conclusion, this study has shown encouraging results for flow-based ASL in both brain and kidney. Flow-based ASL provides a promising planning-free and transit time-insensitive alternative for spatially selective ASL in subjects with slow flow. VSI-ASL, as flow-based ASL technique, shows the most promising results. In brain, VSI-ASL has a similar performance as the standardized pCASL, although in kidney more technical development at 3T (ie, reduction of B_1-sensitivity) is necessary to match the performance of FAIR.

ACKNOWLEDGMENTS

CONFLICT OF INTEREST

M.J.P.v.O. receives research support from P.M.v.S. is co-founder and shareholder of MRIguidance BV.

ORCID

Suzanne L. Franklin https://orcid.org/0000-0001-6886-5578
Isabell K. Bones https://orcid.org/0000-0002-7916-5013
Anita A. Harteveld https://orcid.org/0000-0002-3379-0710
Lydiane Hirschler https://orcid.org/0000-0003-2379-0861
Qin Qin https://orcid.org/0000-0002-6432-2944
Johannes M. Hoogduin https://orcid.org/0000-0001-7707-0750
Clemens Bos https://orcid.org/0000-0002-9246-3242
Matthias J. P. van Osch https://orcid.org/0000-0001-7034-8959
Sophie Schmid https://orcid.org/0000-0003-0750-7798

REFERENCES

1. Alsop DC, Detre JA, Golay X, et al. Recommended implementation of arterial spin-labeled perfusion MRI for clinical applications: A consensus of the ISMRM perfusion study group and the European consortium for ASL in dementia. *Magn Reson Med*. 2015;73:102-116.

2. Qiu D, Straka M, Zun Z, Bammer R, Moseley ME, Zaharchuk G. CBF measurements using multidelay pseudocontinuous and velocity-selective arterial spin labeling in patients with long arterial transit delays: Comparison with xenon CT CBF. *J Magn Reson Imaging*. 2012;36:110-119.

3. Bolar DS, Gagoski B, Orbach DB, et al. Comparison of CBF measured with combined velocity-selective arterial spin-labeling and pulsed arterial spin-labeling to blood flow patterns assessed by conventional angiography in pediatric Moyamoya. *Am J Neuroradiol*. 2019;40:1842-1849.

4. Shin T, Worters PW, Hu BS, Nishimura DG. Non-contrast-enhanced renal and abdominal MR angiography using velocity-selective inversion preparation. *Magn Reson Med*. 2013;69:1268-1275.

5. Bones IK, Franklin SL, Harteveld AA, et al. Influence of labeling parameters and respiratory motion on velocity-selective arterial spin labeling for renal perfusion imaging. *Magn Reson Med*. 2020;84:1919-1932.

6. Dai W, Fong T, Jones RN, et al. Effects of arterial transit delay on cerebral blood flow quantification using arterial spin labeling in an elderly cohort. *J Magn Reson Imaging*. 2017;45:472-481.

7. Togao O, Hiwatashi A, Obara M, et al. Acceleration-selective arterial spin-labeling MR angiography used to visualize distal cerebral arteries and collateral vessels in moyamoya disease. *Radiology*. 2018;286:611-621.

8. Safian RD, Textor SC. Renal-artery stenosis. *N Engl J Med*. 2001;344:431-442.

9. Edelman RR, Koktzoglou I. Noncontrast MR angiography: An update. *J Magn Reson Imaging*. 2019;49:355-373.

10. Jahanian H, Noll DC, Hernandez-Garcia L. B0 field inhomogeneity considerations in pseudo-continuous arterial spin labeling (pCASL): Effects on tagging efficiency and correction strategy. *NMR Biomed*. 2011;24:1202-1209.

11. Greer JS, Wang Y, Pedrosa I, Madhuranthakam AJ. Pseudo-continuous arterial spin labeled renal perfusion imaging at 3T with improved robustness to off-resonance. *Proc Int Soc Magn Reson Med Montr Canada*. 2019;27:4959.

12. Selby NM, Blankestijn PJ, Boor P, et al. Magnetic resonance imaging biomarkers for chronic kidney disease: A position paper from the European cooperation in science and technology action PARENCHIMA. *Nephrol Dial Transplant*. 2018;33(suppl_2):ii4-ii14.

13. Odudu A, Nery F, Harteveld AA, et al. Arterial spin labelling MRI to measure renal perfusion: A systematic review and statement paper. *Nephrol Dial Transplant*. 2018;33:15-21.

14. Nery F, Buchanan CE, Harteveld AA, et al. Consensus-based technical recommendations for clinical translation of renal ASL MRI. *Magn Reson Mater Physics, Biol Med*. 2020;33:141-161.

15. Norris DG, Schwarzbauer C. Velocity selective radiofrequency pulse trains. *J Magn Reson*. 1999;137:231-236.

16. Wong EC, Cronin M, Wu W-C, Inglis B, Frank LR, Liu TT. Velocity-selective arterial spin labeling. *Magn Reson Med*. 2006;55:1334-1341.

17. Schmid S, Ghariq E, Teeuwisse WM, Webb A, van Osch MJP. Acceleration-selective arterial spin labeling. *Magn Reson Med*. 2014;71:191-199.

18. Guo J, Wong EC. Increased SNR efficiency in velocity selective arterial spin labeling using multiple velocity selective saturation modules (mm-VSASL). *Magn Reson Med*. 2015;74:694-705.

19. Qin Q, van Zijl PCM. Velocity-selective-inversion prepared arterial spin labeling. *Magn Reson Med*. 2016;76:1136-1148.

20. Schmid S, Petersen ET, Van Osch MJP. Insight into the labeling mechanism of acceleration selective arterial spin labeling. *Magn Reson Mater Physics, Biol Med*. 2016;30:165-174.

21. Ogg RJ, Kingsley PB, Taylor JS. WET, a T1- and B1-insensitive water-suppression method for in vivo localized 1H NMR spectroscopy. *J Magn Reson Ser B*. 1994;104:1-10.

22. Golay X, Petersen ET, Hui F. Pulsed star labeling of arterial regions (PULSAR): A robust regional perfusion technique for high field imaging. *Magn Reson Med*. 2005;53:15-21.

23. Bones IK, Harteveld AA, Franklin SL, et al. Enabling free-breathing background suppressed renal pCASL using fat imaging and retrospective motion correction. *Magn Reson Med*. 2019;82:276-288.

24. Harteveld AA, de Boer A, Franklin SL, Leiner T, van Stralen M, Bos C. Comparison of multi-delay FAIR and pCASL labeling approaches for renal perfusion quantification at 3T MRI. *Magn Reson Mater Physics, Biol Med*. 2019;33:81-94.

25. Luh W, Wong EC, Bandettini PA, Hyde JS. QUIPSS II with thin-slice TI1 periodic saturation: A method for improving accuracy of quantitative perfusion imaging using pulsed arterial spin labeling. *Magn Reson Med*. 1999;41:1246-1254.

26. Clare S, Jezzard P. RapidT1 mapping using multislice echo planar imaging. *Magn Reson Med*. 2001;45:630-634.

27. Yarnykh VL. Actual flip-angle imaging in the pulsed steady state: A method for rapid three-dimensional mapping of the transmitted radiofrequency field. *Magn Reson Med*. 2007;57:192-200.

28. Penny W, Friston K, Ashburner J, Kiebel S, Nichols T. *Statistical Parametric Mapping: The Analysis of Functional Brain Images*. Amsterdam: Elsevier Ltd; 2007.

29. Ritter F, Boskamp T, Homeyer A, et al. Medical image analysis. *IEEE Pulse*. 2011;2:60-70.

30. Huizinga W, Poot D, Guyader J-M, et al. PCA-based groupwise image registration for quantitative MRI. *Med Image Anal*. 2016;29:65-78.

31. Meakin JA, Jezzard P. An optimized velocity selective arterial spin labeling module with reduced eddy current sensitivity for improved perfusion quantification. *Magn Reson Med*. 2013;69:832-838.

32. Guo J, Meakin JA, Jezzard P, Wong EC. An optimized design to reduce eddy current sensitivity in velocity-selective arterial spin labeling using symmetric BIR-8 pulses. *Magn Reson Med*. 2015;73:1085-1094.

33. Hernandez-Garcia L, Nielsen J-F, Noll DC. Improved sensitivity and temporal resolution in perfusion FMRI using velocity selective inversion ASL. *Magn Reson Med*. 2018;81:1004–1015.

34. Pallone TL, Edwards A, Mattson DL. Renal medullary circulation. *Compr Physiol*. 2012;2:97-140.

35. Robson PM, Madhuranthakam AJ, Dai W, Pedrosa I, Rofsky NM, Alsop DC. Strategies for reducing respiratory motion artifacts in renal perfusion imaging with arterial spin labeling. *Magn Reson Med*. 2009;61:1374-1387.

36. Franklin SL, Schmid S, Bos C, van Osch MJP. Influence of the cardiac cycle on velocity selective and acceleration selective arterial spin labeling. *Magn Reson Med*. 2020;83:872-882.

37. Echeverria-Chasco R, Vidorreta M, Aramendía-Vidaurreta V, Cano D, Escalada J, Garcia-Fernandez N, Bastarrika G, Fernández-Seara MA. Optimization of pseudo-continuous arterial spin labeling for renal perfusion imaging. *Magn Reson Med*. 2021;85:1507-1521.

SUPPORTING INFORMATION

Additional Supporting Information may be found online in the Supporting Information section.

FIGURE S1 Data from a subject with severely affected VSI-ASL images (vol 1) and a subject with minimally affected VSI-ASL images (vol 2). A B_1-map, including an overlay of the kidney contours, a VSI-ASL image with background suppression (BGS) and a VSI-ASL image without BGS are shown. Vol 1 shows clear negative signal in the VSI-ASL image. This artefact co-localizes with areas with reduced B_1-power in the B_1-map. Performing VSI-ASL without BGS showed less artefacts, although in that image there is still spatial variation of the VSI-ASL image. This indicates that the VSI-ASL artefacts are related to the B_1-sensitivity of the BGS-pulses as well as the pulses in the VSI-ASL modules. These VSI-ASL images were acquired with 10 repetitions

FIGURE S2 Simulation of the resulting ASL-signal for the whole VSI-sequence using three different background suppression (BGS) settings; with 3 BGS-pulses, with 2 BGS-pulses and without any BGS-pulses. Data was simulated using the settings for kidney, as described in the main paper. Simulation was done for a range of B_0-values (top row) and a range of B_1-values (bottom row). Results indicate that for VSI with 3 BGS-pulses and to a lesser degree VSI with 2 BGS-pulses negative signal can be expected for low B_1-values (<0.5)

FIGURE S3 For all ASL-techniques the temporal signal-to-noise ratio (tSNR) in a) kidney cortex and b) kidney medulla using all voxels inside the mask, ie, without excluding the artifact observed in VSI-ASL

FIGURE S4 (A) T1-weighted scan for all five subjects. Subject 5 appears to have a deviating CSF-system with larger ventricles than the other subjects. (B) perfusion-weighted signal (PWS) in the gray matter mask. Columns represent the five subjects, and rows the five ASL-techniques. One slice in the middle of the brain is shown

FIGURE S5 For all ASL-techniques the (A) ASL-signal of gray matter, treated as direct indicator of spatial signal-to-noise ratio (SNR) and (B) temporal standard deviation (tSTD) in the gray matter in brain